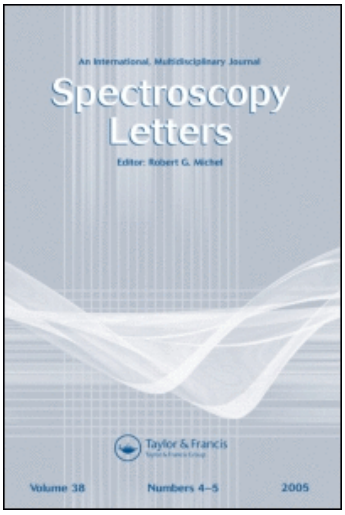

Spectroscopy Letters
Publication details, including instructions for authors and subscription information:
http://www.informaworld.com/smpp/title~content=t713597299

Ellipsometry, FTIR, Raman and X-Ray Spectroscopy Analysis of PECVD a-$Si_{1-x}C_x$:H Film

Rongdun Hong[a]; Jun Huang[a]; Xiaping Chen[a]; Yi Zhou[b]; Dayi Liu[c]; Zhengyun Wu[a]
[a] Physics Department, Xiamen University, Xiamen, People's Republic of China [b] Electrical Engineering Department, University of California, Los Angeles, California, USA [c] Semiconductor Photonics Research Center, Xiamen University, Xiamen, People's Republic of China

Online publication date: 27 April 2010

To cite this Article Hong, Rongdun , Huang, Jun , Chen, Xiaping , Zhou, Yi , Liu, Dayi and Wu, Zhengyun(2010) 'Ellipsometry, FTIR, Raman and X-Ray Spectroscopy Analysis of PECVD a-$Si_{1-x}C_x$:H Film', Spectroscopy Letters, 43: 4, 298 — 305
To link to this Article: DOI: 10.1080/00387010903348276
URL: http://dx.doi.org/10.1080/00387010903348276

Spectroscopy Letters, 43:298–305, 2010

ISSN: 0038-7010 print/1532-2289 online
DOI: 10.1080/00387010903348276

Taylor & Francis
Taylor & Francis Group

Ellipsometry, FTIR, Raman and X-Ray Spectroscopy Analysis of PECVD a-$Si_{1-x}C_x$:H Film

Rongdun Hong[1], Jun Huang[1], Xiaping Chen[1], Yi Zhou[2], Dayi Liu[3], and Zhengyun Wu[1]

[1]Physics Department, Xiamen University, Xiamen, People's Republic of China
[2]Electrical Engineering Department, University of California, Los Angeles, California, USA
[3]Semiconductor Photonics Research Center, Xiamen University, Xiamen, People's Republic of China

ABSTRACT Hydrogenated amorphous silicon carbide (a-$Si_{1-x}C_x$:H) films were deposited by RF plasma enhanced chemical vapor deposition (PECVD) and subsequently annealed in N_2 atmosphere at different temperatures. Systematic investigations of the deposition temperature and annealing effect on the film's properties, including film thicknesses, optical bandgap, refractive indexes, absorption coefficient (α), chemical bond configurations, stoichiometry and crystalline structures, were performed using ellipsometry, FTIR absorbance spectroscopy, Raman spectroscopy, XPS, and XRD. All of the results indicate that the structural and optical properties of the a-$Si_{1-x}C_x$:H film can be effectively engineered by proper annealing conditions. Moreover, molecular vibrational level equation was introduced to explain the peak shift detected by FTIR and Raman spectroscopy.

KEYWORDS a-$Si_{1-x}C_x$:H, ellipsometry, FTIR, PECVD, raman, XPS, XRD

1. INTRODUCTION

For high-power, high-temperature and high-frequency applications, wide bandgap semiconductors are the most attractive alternatives for Si because of the inherent material advantages such as larger bandgap, higher breakdown field, and higher saturation electron drift velocity. Among all the wide bandgap semiconductors, SiC stands out as a promising candidate for harsh environment applications, not only for its chemical and thermal stability but also for its eminent mechanical and electrical properties. Furthermore, SiC has many advantages over other wide bandgap semiconductors, such as having a stable thermally grown Si_xO_{1-x} with a relatively low interface trap density, low particle diffusion coefficient, high thermal conductivity[1–3] and the low lattice mismatch with Si, which allows for epitaxy growth of SiC film on Si substrate.

There are several methods to grow SiC material, including physical vapor transport (PVT)[4] and metal organic chemical vapor deposition (MOCVD)[5] for single-crystal SiC, low-pressure chemical vapor deposition (LPCVD) for SiC polycrystal film,[6] plasma enhanced chemical vapor deposition (PECVD) for amorphous $Si_{1-x}C_x$:H films.[7] Unlike other growth methods, PECVD can

Received 22 June 2009; accepted 18 September 2009.

Address correspondence to Zhengyun Wu, Physics Department, No. 422 Siming South Road, Xiamen 361000, China. E-mail: zhywu@xmu.edu.cn

be processed at much lower temperature, which ranges from 200°C to 500°C. And amorphous SiC has many applications in microelectronic and optoelectronic devices. For example, it can be used as conductive diffusion barrier layer, anti-reflection coating and passivation layer in thin film solar cell,[8] MEMS device[9] and waveguide.[10] Moreover, the amorphous $Si_{1-x}C_x$:H films are more suitable than the crystalline SiC for the mechanical process.[11]

It is noted that the optical bandgap, chemical inertness and hardness of a-Si_xC_{1-x}:H can be tuned by the annealing and deposition conditions such as the temperature, the elements proportion Si/C, hydrogen content and annealing atmosphere. And these properties of a-Si_xC_{1-x}:H are crucial to the device performance. The emphasis of this work is to investigate the structural and optical properties of amorphous SiC films grown at different temperature (T_d) and annealing effect on these properties.

2. EXPERIMENT DETAILS

P type, (100) oriented Silicon wafers with a resistivity of 8 to 12 $\Omega \cdot$cm were used as the substrate. The substrate was cleaned with the RCA procedure, dipped in a 2% hydrofluoric solution for about 2 minutes to remove native oxide, rinsed in deionized water, and finally blown dry using nitrogen. It is then immediately loaded into the PECVD chamber, which is equipped with an RF power source with an operating frequency of 13.56 MHz and a power density of $0.45\,W/cm^2$. After the temperature in the chamber was stabilized at the designed one, a turbo molecular pump and rotary pump were used to maintain the chamber pressure of 7×10^{-4} Pa. Then SiH_4 and CH_4 gases were introduced into the chamber. The pressure in the chamber was kept at 3 Pa during the deposition. And the flow rates of SiH_4 (diluted to 5% in Ar_2) and CH_4 were 60 sccm and 12 sccm, respectively. Time for deposition was 30 minutes for all samples and the deposition temperatures (T_d) were 330°C, 370°C, 400°C and 460°C for sample S1, S2, S3 and S4, respectively. After the deposition was done, the samples were annealed at 650°C, 800°C, 950°C and 1100°C, respectively, in N_2 atmosphere for 30 minutes. Finally, the samples were dipped into 2% HF acid for about 2 minutes to remove the surface oxide layer. The thicknesses and extinction coefficient k of the samples were measured by Uvisel FUV ellipsometer from Horiba Jobin Yvon, France. Then Samples' optical bandgap was deduced from k. FTIR absorbance spectroscopy and Raman Spectroscopy were used to characterize the chemical bond configuration and structure of the films. The scanned range of FTIR is 400 to 4000 cm^{-1} in the absorption mode with a resolution of 1 cm^{-1}, and the Raman shift range was 200 to 2200 cm^{-1}, with a 325 nm line of a 10 mW He–Ne laser as the exciting source. Quantum 2000 Scanning ESCA Microprobe (Philadelphia, USA) was used for the XPS analysis of the films up to a 100 nm depth, then the stoichiometry of Si/C was calculated. Finally, the structures of films were analyzed by X-ray diffraction (XRD) equipment from PAN algtical X'pert PRO, Holland.

3. RESULTS AND DISCUSSION

3.1. Ellipsometry Results

The thicknesses of SiC films deposited at different temperatures were measured by an Uvisel FUV ellipsometer (France). Then the deposition rates were calculated, which were shown in Fig. 1(a). The rate decreased with the deposition temperature (T_d), which was similar to the result of the other work.[12] According to M. Losurdo, the optical bandgap depends not only on the overall C content, but also on the microstructure and Si-C bond configuration, which will reduce the deposition rate.[13] However the structure of the deposited samples before annealing may be almost the same, for the Tauc plots of all deposited sample are identical (Fig. 2a). Moreover XRD result also shows that the structures of all samples as-deposited are almost the same. So, the reason for the decrease of the deposition rate may be that more bonds of C-H and Si-H of the reaction gas are broken at higher T_d, resulting in a low H content in the sample (Proved by the FTIR Fig. 3(a)). So, deposition rate will decrease with T_d.

Fig. 1(b) shows the thicknesses of sample S2 after being annealed at different temperatures (T_a). The film is thinner as T_a become higher. This may be caused mainly by the loss of H during annealing and the change of the film structure such as bond reconfiguration and crystallization, which are revealed by FTIR and XRD analysis (See Fig. 3a and Fig. 7).

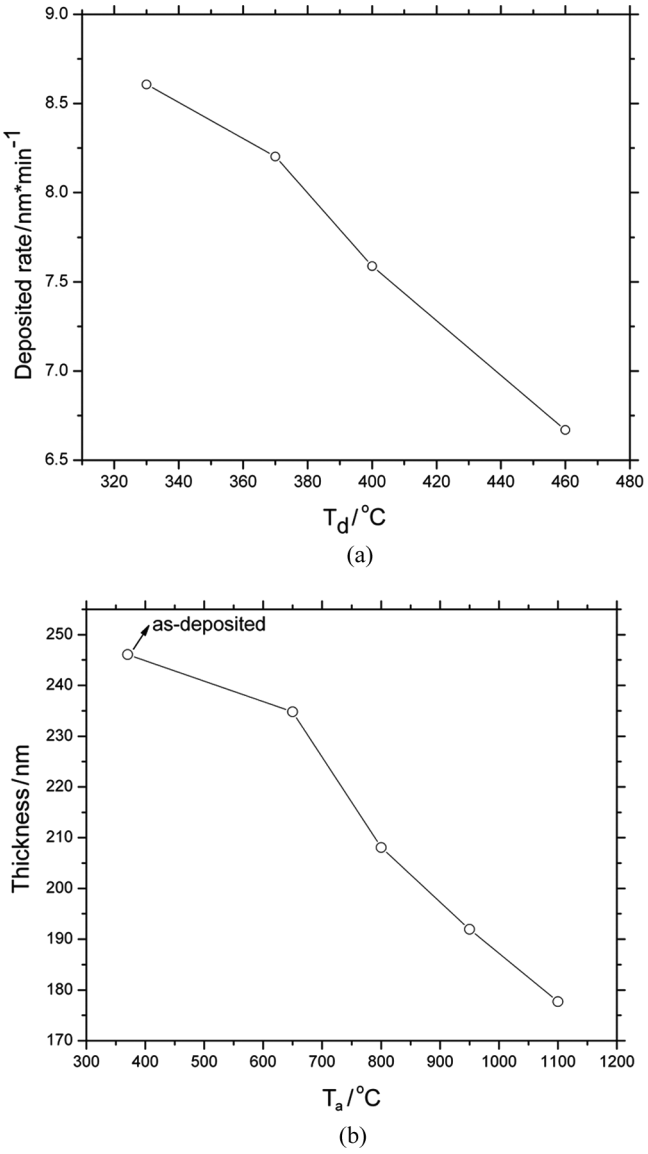

FIGURE 1 **(a) Deposited rates of PECVD a-$Si_{1-x}C_x$:H films at different T_d. (b) Thicknesses of sample S2 as-deposited and after annealing. The deposited rate decreases with T_d and the thickness of S2 also decreases with annealing temperature.**

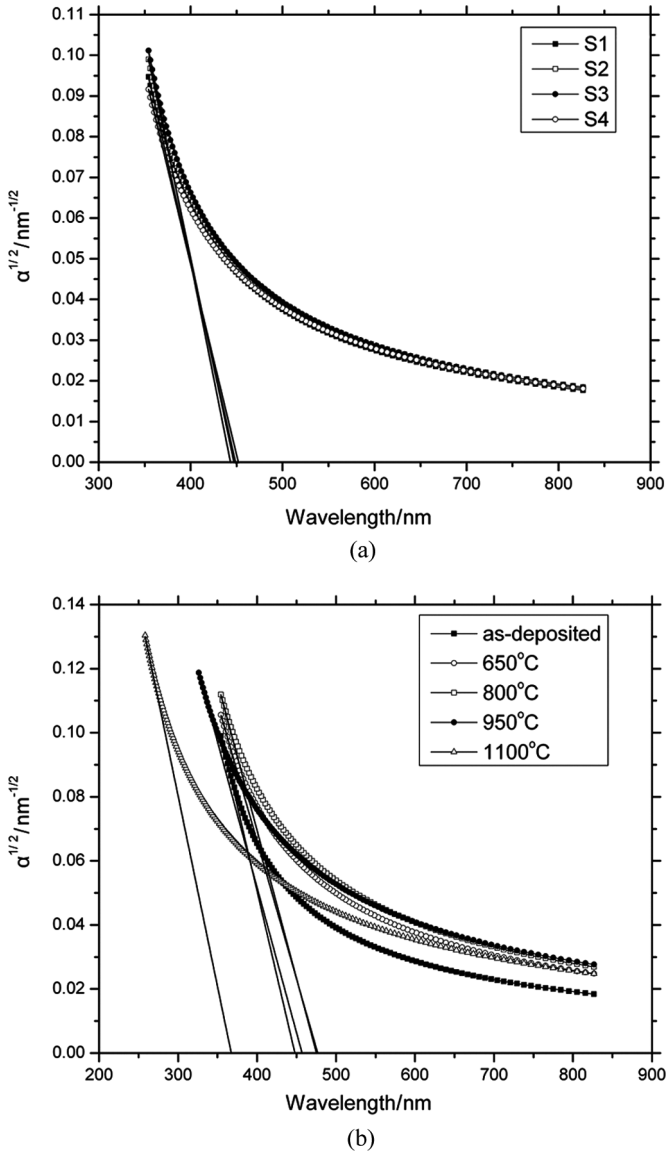

FIGURE 2 **(a) Tauc's plot of $a^{1/2}$ versus wavelength for as-deposited samples. (b) Tauc's plot of sample S2 as-deposited and annealed at different T_a. There is little change on samples' optical bandgap (E_g) related to T_d. However, high annealing temperature has a significant effect on the E_g. E_g increase a lot after 1100°C annealing.**

Equation (1) is used to calculate the absorbance index a from the extinction coefficient k measured by ellipsometry. For SiC, an indirect bandgap semiconductor, the relation between a and hv is shown in Eq. (2), where λ_0 is wavelength; B_d is a constant; E_g is sample's optical bandgap; hv is the energy of photon.

$$a = 4\pi k/\lambda_0 \tag{1}$$

$$ahv = B_d(hv - E_g)^2 \tag{2}$$

Tauc's plot[14] of $a^{1/2}$ versus wavelength and Eq. (3) (where λ_c is the cutoff wavelength) were combined to reveal the trend of the change of samples' optical bandgap E_g with annealing temperature, as illustrated in Fig. 2(a). For all samples, the λ_c are almost the same, which are about 450 nm corresponding to E_g around 2.76 eV.

$$E_g = \frac{1.24}{\lambda_c} \tag{3}$$

The Tauc's plots of sample S2 as-deposited and annealed at different T_a are presented in Fig. 2(b). Although the Tauc approach only provide a rough

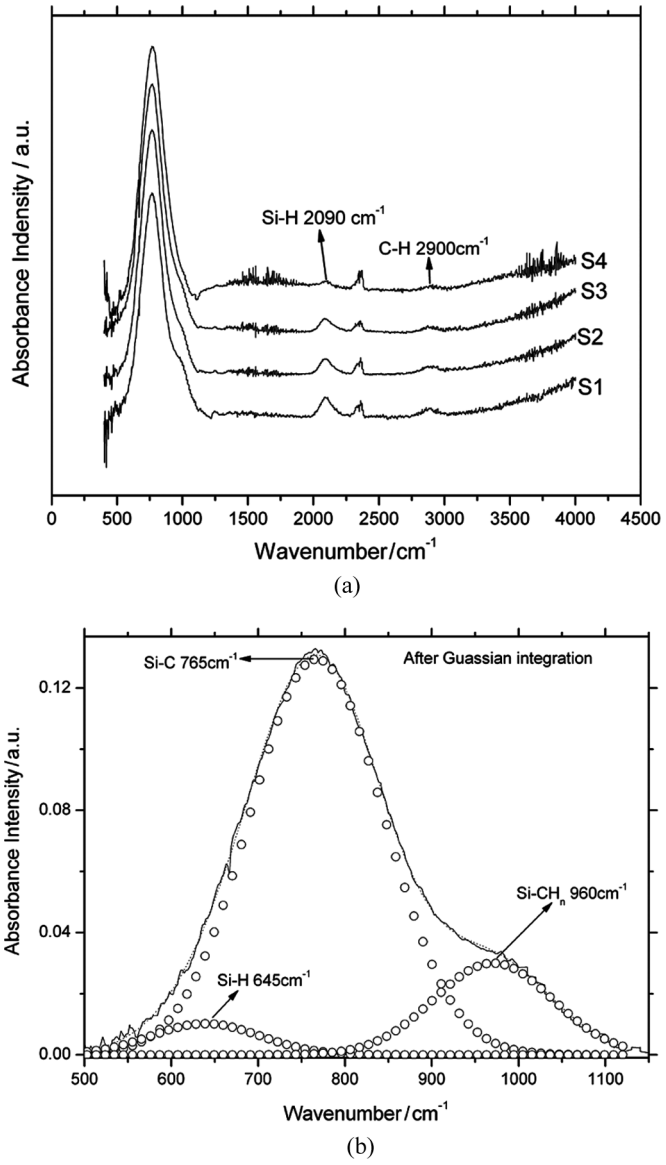

FIGURE 3 **(a) FTIR absorbance spectrum of the samples at different T_d. (b) Three bands, for Si-H (645 cm^{-1}), Si-C (765 cm^{-1}) and a combination of C-SiH_n and the Si-CH_n (960 cm^{-1}), are obtained by Gaussian integration from the FTIR band of 500 to 1120 cm^{-1}.**

estimation of the optical bandgap of the samples studied in this paper, the trend of E_g still can be obtained. After annealed at 650°C, E_g of S2 decreases from 2.77 eV to 2.61 eV, and it increases with T_a from 2.61 eV to 3.37 eV. There is a sharp change of the E_g when T_a reaches 1100°C. This result is similar to the change of Si-C density with annealing temperature in FTIR spectra (Fig. 5). Therefore we conclude that the change of E_g after annealing was attributed to the change of bond configuration and microstructure,[13] especially when T_a is high enough.

3.2. FTIR Absorbance and Raman Spectroscopy Analysis

Fig. 3(a) presents the FTIR absorbance spectra of the samples grown at different T_d. The wavenumbers of peaks for all four lines are similar. There are four main absorbance bands in the spectra, which are from 500 to 1120 cm^{-1}, 1980 to 2230 cm^{-1}, 2280 to 2400 cm^{-1}, and 2730 to 3080 cm^{-1}. It was found that the band around 2280 to 2400 cm^{-1} fluctuated during the experiment for each sample. This band was assigned as the CO_2 vibration band.[15] The fluctuation of this peak might be due to the fluctuation of the CO_2 concentration in the atmosphere. It was reported that two bands for Si-H at 2000 to 2250 cm^{-1} and 550 to 700 cm^{-1} were characteristic of the vacancy-type complexes, while bands between 1900 to 2000 cm^{-1} and 700 to 800 cm^{-1} were attributed to interstitial—type complexes.[16] However, in our work, no peak at 1900 to 2000 cm^{-1} was detected by FTIR, which suggests that the Si-H interstitial-type complexes have a much lower concentration or do not exist in the sample. In conclusion, the main chemical bonds located between 500 cm^{-1} and 1120 cm^{-1} are a combination of C-SiH_n and the Si-CH_n, Si-H vacancy type complexes and Si-C. Gaussian integration was used to separate the band of 500 to 1120 cm^{-1} into three bands, which were around 500 to 850 cm^{-1}, 530 to 1000 cm^{-1}, and 730 to 1120 cm^{-1} with peaks of about 645 cm^{-1}, 765 cm^{-1}, and 960 cm^{-1} (Fig. 3b), respectively. Those peaks are for wagging mode of Si-H, stretching mode of Si-C, and a combination of C-SiH_n stretching mode and the Si-CH_n stretching mode. The peaks around 2090 cm^{-1} and 2900 cm^{-1} are for the stretching mode of Si-H and C-H bonds.[16–18]

Because the 960 cm^{-1} peak disappeared after annealing (see Fig. 5), we think that this peak may be the stretching mode of combination of C-SiH_n and Si-CH_n. The disappearance of this peak could be due to the escape of H atom during annealing. Hooke's law and formula of molecular vibrational level were used for verification. Figure 4 illustrates the Si-$CHSi_2$ cluster and Si-CSi_3 cluster, in which m_1, m_2, and m_3 are the masses of Si atom, $CHSi_2$ cluster and CSi_3 cluster, respectively.

The vibration frequency of the chemical bond can be calculated by Eq. (4) and the vibration absorbance energy can be deduced by Eq. (5), where the

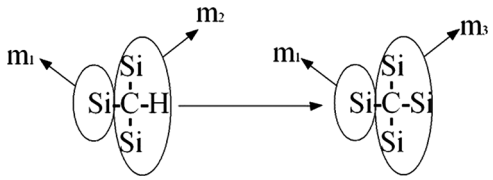

FIGURE 4 Sketch of $Si\text{-}CHSi_2$ cluster and $Si\text{-}CSi_3$ cluster. When H atom changes to Si atom, the bond of Si-C also changes.

k, h, v, and ΔE are elastic coefficient of chemical bonds, Planck constant, vibration frequency and vibration absorbance energy, respectively. Since $m_2 < m_3$, ΔE of $Si\text{-}CHSi_2$ bond is larger than that of $Si\text{-}CSi_3$. Therefore the IR absorbance peak of Si-C bond in $Si\text{-}CHSi_2$ has a blue-shift, which means the peak's wavenumber of Si-C IR absorbance peak in $Si\text{-}CHSi_2$ is larger than that in $Si\text{-}CSi_3$.

$$v = \frac{1}{2\pi}\sqrt{\frac{k}{u}}\left(u = \frac{m_1 m_2}{m_1 + m_2}\right) \tag{4}$$

$$\Delta E = hv = \frac{h}{2\pi}\sqrt{\frac{k}{u}} \tag{5}$$

The areas of bands were calculated to illuminate the effect of deposition temperature on the bonds content in the film (Table 1). Because of the different film thickness, the relative area ratios of FTIR spectra were used to analyze the bonds content in the film. A1 is defined as the sum of areas for the Si-C bond, A2 is for the $C\text{-}SiH_n$ and $Si\text{-}CH_n$ bonds, and A3 is for the Si-H and C-H bonds. From Table 1, the ratios of A1/A2 and A1/A3 become higher at higher T_d, which means the H content in the film decreases and the content of Si-C increases with T_d.

Figure 5 shows the FTIR absorbance spectra (ranging from 500 cm^{-1} to 1300 cm^{-1}) of sample S2 as-deposited and annealed at different T_a. The peak, which is located at 765 cm^{-1}, intensity of Si-C and

TABLE 1 The Areas of Bands in FTIR Spectrum for Samples, Indicating H Content in the Film Decreases and the Content of Si-C Increases with T_d

Sample \ Area	A1(a.u.)	A2(a.u.)	A3(a.u.)	A1/A2	A1/A3
S1	30.3	2.74	0.558	11.0	54.3
S2	32.8	2.20	0.485	14.9	67.6
S3	33.6	0.941	0.431	35.8	78.1
S4	34.9	0.712	0.308	49.0	113

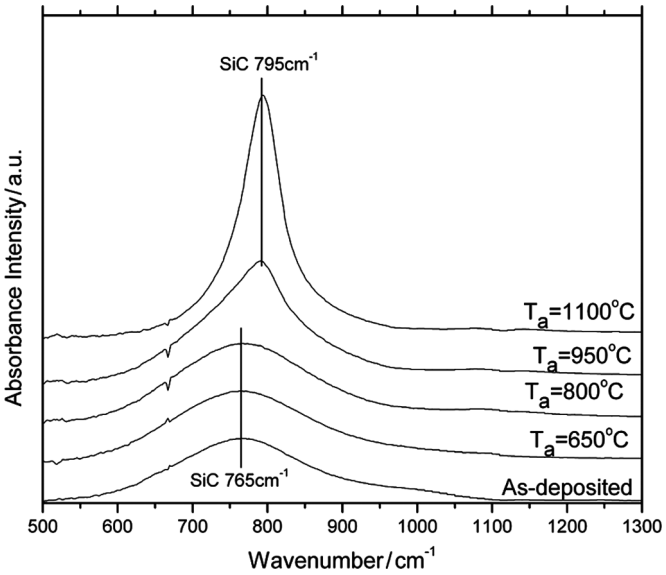

FIGURE 5 FTIR absorbance spectrum (500 to 1300 cm^{-1}) of sample S2 as-deposited and annealed at different T_a. Due to the change of the bonds and structure, there is a blue shift for the absorbance wavenumber of Si-C bond's peak and the Si-C bond absorbance intensity increases at T_a higher than 950°C.

FWHM of Si-C bond decreases with T_a. And there is no shift of the peak associated with the Si-C absorbance wavenumber when T_a is lower than 800°C. However, after being annealed at 950°C and 1100°C, the peaks shift to about 795 cm^{-1}. The blue shift of Si-C peak can also be explained by the Hooke's law and the equation of molecular vibrational level. Since the electron binding energy of C-H (13 eV) is higher than that of Si-H (8 eV), C-H is harder to break than Si-H and the concentration of C-H will be far more than that of Si-H in sample.[19] According to the XPS analysis, the stoichiometric of the sample is $C:Si \approx 1:1$. Therefore there should be some Si-Si-C bonds in film. Since the crystallization temperature of thermal annealing for Si nanocrystal is between 900–1000°C.[20] After being annealed at enough high temperature, some of the Si element in film will form Si crystal, which is verified by the Raman spectroscopy (Fig. 6). As a result, the Si-Si-C bond turns to C-Si-C, leading to the blue shift of Si-C's peak in FTIR. And after being annealed at more than 650°C, the Si-H and C-H peaks at about 2090 cm^{-1} and 2900 cm^{-1} were hardly observed.

So, the FTIR spectra illustrate the intensity of Si-H, C-H and $Si\text{-}CH_n$ in the film decreases, the intensity of Si-C increases and bond configuration also changes with T_a, which explained why the IR peak at 795 cm^{-1} for sample annealed at 1100°C was sharper

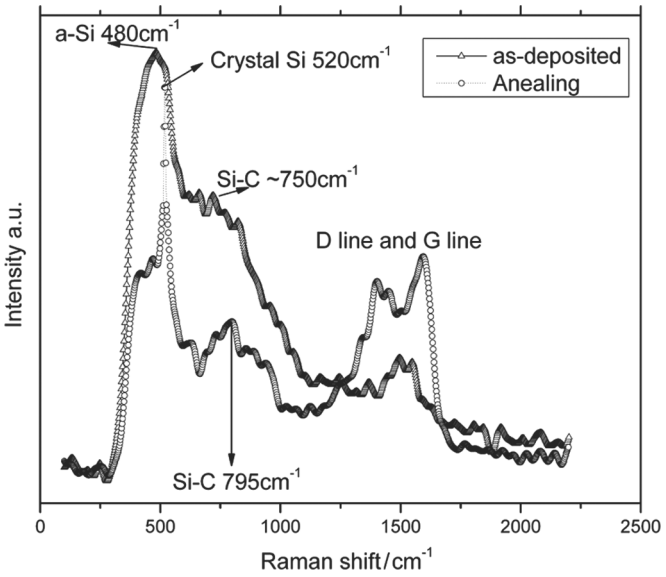

FIGURE 6 **Spectra of Raman shift for sample S3 as-deposited and annealed at 1100°C. Blue shift for Si-C peak can also be seen.**

and the FWHM is smaller than that annealed at 950°C.

Figure 6 shows the Raman shift spectra of sample S2 as-deposited and annealed at 1100°C, displaying two main bands located at 400 to 1000 cm^{-1} and 1380 to 1670 cm^{-1}, respectively The broad peak at about 480 cm^{-1} corresponds to amorphous Si; the peak at around 750 cm^{-1} is for amorphous SiC and the small peak at about 1500 cm^{-1} is for C-C bonds. After annealing, the peak for amorphous Si disappears and there is a sharper peak around 520 cm^{-1} accompanied by a shoulder at 480 cm^{-1}. These two peaks are for the combination of amorphous Si and crystal Silicon.[21] The peak for Si-C bond is sharper and shifts to 795 cm^{-1}, which is attributed to the TO mode of phonon absorption.[22] The peak for C-C splits into two peaks at around 1400 cm^{-1} and 1590 cm^{-1}, corresponding to the D line disordered structure and G line of the graphite structure,[23] respectively Thus, after being annealed at 1100°C, there is not only silicon but C-C bonds formed in the film and the arrangement of atoms in SiC film is reordered. However, it should be noted that the contents of Si-Si bonds and C-C bonds are rather small as compared to the Si-C bond, which is evidenced by the XPS analysis.

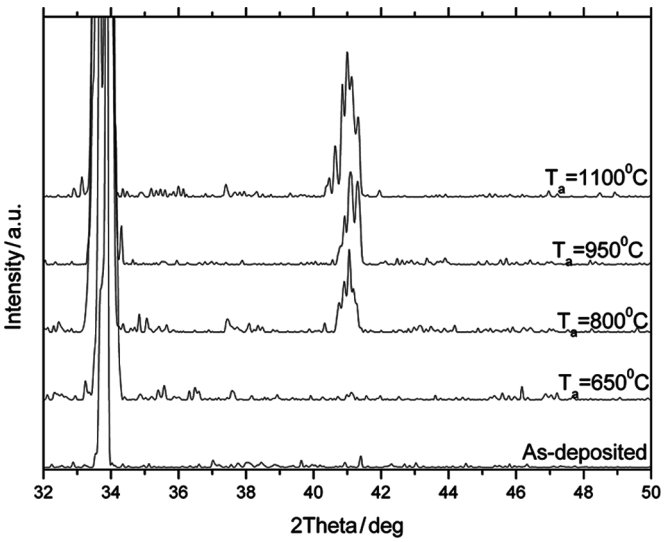

FIGURE 7 **XRD spectra for sample S4 as-deposited and annealed at different T_a. It proves there is SiC crystal (002) after annealing at a certain temperature and the intensity for SiC crystal (002) increases with T_a.**

3.3. XRD and XPS Analysis

Graze Angle XRD was used for the structure analysis. Figure 7 shows a series of XRD spectra for sample S4 as-deposited and annealed at different T_a for 30 minutes, with a 2θ range from 32° to 50°.

S4 was chosen for this analysis because there is less H atom in sample S4 as-deposited, which may have less additional effect on the XRD and XPS result. For the as-deposited sample, only one peak at around 34° was seen, which is attributed to the Si (002)[7] from the substrate. With the increase of annealing temperature from 650°C to 1100°C, there is a significant enhancement of 3C-SiC (002) diffraction peak, which is located at about $\theta = 41°$. The higher annealing temperature does show a positive effect on the crystallization of the a-$Si_{1-x}C_x$:H film.

All the XPS spectra have been fitted with the removal of a linear background and by a Gaussian Function. Equation (7) was used to calculate the stoichiometry, where X, A_x, and S_x are the sample's atom, the area under the peak and the sensitivity factor for X, respectively. The sensitivity factors for carbon and silicon are 0.31 and 0.37, respectively.[24]

$$\%X = \frac{\left(\frac{A_X}{S_X}\right)}{\sum_{i=1}^{Ai}\left(\frac{Ai}{Si}\right).} \tag{7}$$

The stoichiometric results (C:Si ≈ 1:1) are quite similar for all the samples before and after annealing. Figure 8 shows the XPS spectra of sample S2 as-deposited and after being annealed at 1100°C,

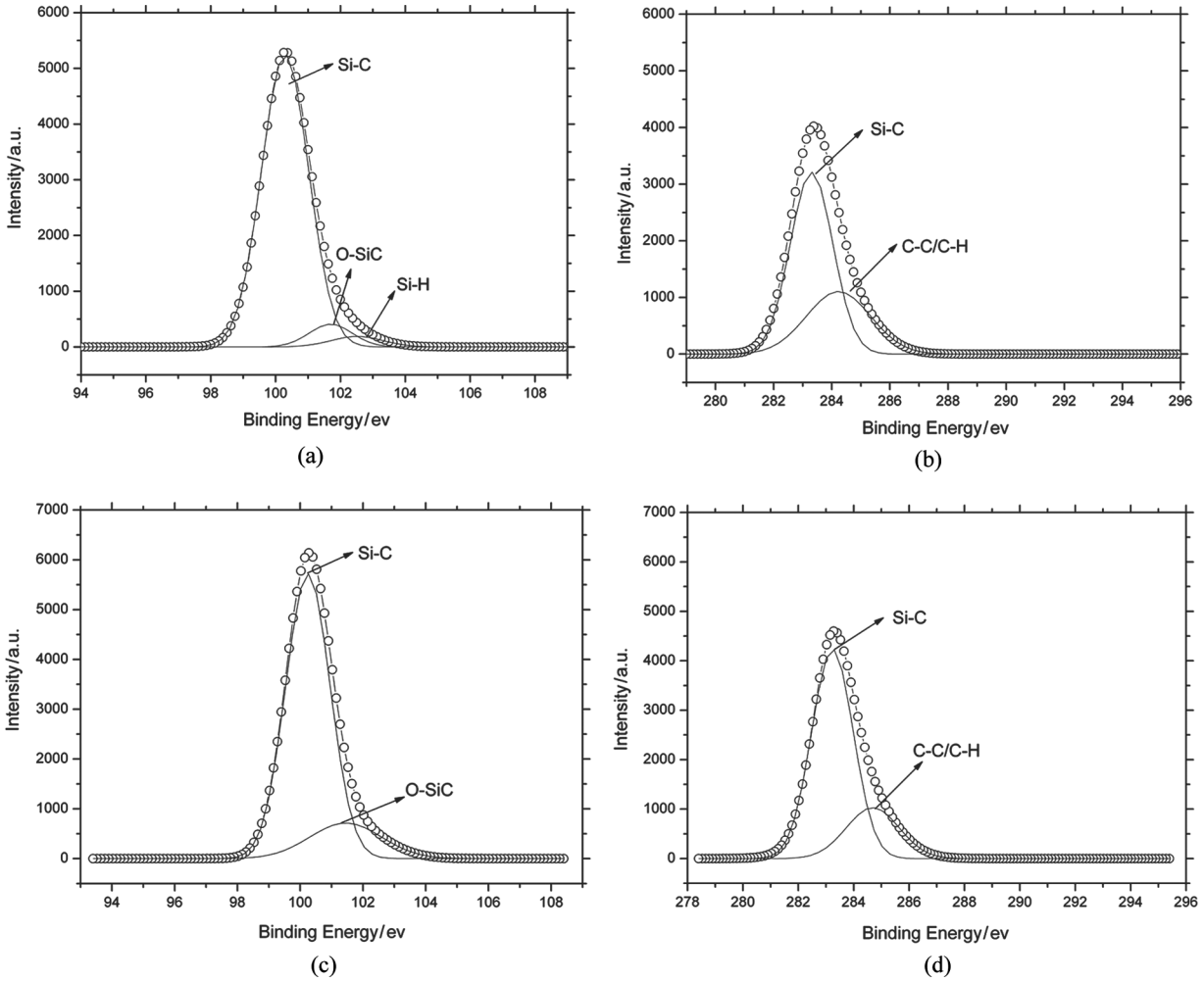

FIGURE 8 XPS spectra for Si_{2p} and C_{1s} of sample S4 as-deposited (a) (b) and annealed at 1100°C (c) (d). C:Si ≈ 1:1. After annealing at 1100°C, O content increase, H content can not be observed and the peak for C-C/C-H shift from 284.1 eV to 284.6 eV means the loss of H content and the increase of C-C.

which are exemplified with the deconvoluted Gaussian peaks.

Compared with the previous report,[25] which shows the peaks for Si_{2p} and C_{1s} for 3C-SiC are located at 100.3 eV and 282.7 eV, the peaks for Si_{2p} and C_{1s} in our experiment of Si-C are at 100.2 eV and 283.2 eV. For sample S4 as-deposited, the peaks at 100.2 eV, 101.6 eV, and 102.5 eV (Figs. 8a and b) are the Si_{2p} peaks for Si-C, O-SiC and H-SiC, respectively. After being annealed at 1100°C, there are still peaks for Si-C and O-SiC, but not for H-SiC (Figs. 8c and d). And the O atom should be induced from the atmosphere of deposition and annealing. Moreover, before and after annealing, although the peak of C_{1s} for Si-C are both located at 283.2 eV, the peak for C-C/C-H shift from 284.1 eV to 284.6 eV. It have been reported that the binding energy for C-H and C-C are 284.1 eV and 284.6 eV,[26,27] respectively. Thus we can conclude, after annealing, the H content is lowered and some C-C are formed in the film, as shown in FTIR and Raman analysis. However, the peak for the C-C/C-H is also partly due to the adventitious C.

4. CONCLUSION

In conclusion, for the a-$Si_{1-x}C_x$:H films in this study, the deposition rates, refractive indexes, absorption coefficient (α) and optical bandgap of the films was characterized by ellipsometry; FTIR absorbance spectroscopy and Raman shift spectroscopy analysis were performed to investigate the chemical bond configurations; Hooke's law and equation of Molecular Vibrational Level equation were introduced to explain the change of chemical bond configuration; and the author also adopted XRD and XPS to analyse the stoichiometry

and crystalline structures of a-$Si_{1-x}C_x$:H films in this paper.

According to the experimental result, the deposited rate decreased with deposition temperature and the thickness of film became thinner at a higher annealing temperature. In this paper, however, the deposition temperature has little effect on the optical and structural characteristics of the a-$Si_{1-x}C_x$:H film, while the annealing has a great effect on the optical bandgap, structure and optical characteristics of it. The H content in the film decreases and the content of Si-C increases with annealing temperature. The optical bandgap varies considerately at different annealing temperature. The XRD SiC crystalline peak increases with the annealing temperature. All of the results indicate that the structural and optical properties of the a-$Si_{1-x}C_x$:H film can be effectively engineered by proper annealing conditions.

REFERENCES

1. Huran, J.; Zaťko, B.; Hotový, I.; Pezoldt, J.; Kobzev, A. P.; Balalykin, N. I. PECVD silicon carbide deposited at different temperature. *Czechoslovak J. Phys.* **2006**, *56*, 1207–1211.
2. Huran, J.; Hotovy, I.; Dubecky, F.; Balalykin, N. I. N doped a-SiC:H Films Deposited by PECVD and Annealed by Pulse Electron Beam. SIMC 13th International Conference, **2004**, 93–97.
3. Afránková, J. Š.; Huran, J.; Hotový, I.; Kobzev, A. P.; Korenev, S. A. Characterization of nitrogen-doped amorphous silicon carbide thin films. *Vacuum* **1998**, *51*, 165–167.
4. Ohtani, N.; Fujimoto, T.; Katsuno, M.; et al. Growth of large high-quality SiC single crystals. *J. Crystal Growth* **2002**, *237*, 1180–1186.
5. Jung, C.-K.; Lim, D.-C.; Jee, H. G.; et al. Hydrogenated amorphous and crystalline SiC thin films grown by RF-PECVD and thermal MOCVD; comparative study of structural and optical properties. *Surface Coatings Technol.* **2003**, *171*, 46–50.
6. Gao, D.; Wijesundara, M. B. J.; Carraro, C.; et al. Recent progress toward a manufacturable polycrystalline SiC surface micromachining technology. *IEEE Sensors J.* **2004**, *14*, 441–448.
7. Tong, L.; Mehregany, M. Amorphous Silicon Carbide Films by Plasma-Enhanced Chemical Vapor Deposition. MEMS'93 *Procc., IEEE,* **1993**, 242–247.
8. Glunz, S. W.; Janz, S.; Hofmann, M.; Roth, T.; Willeke, G. Surface Passivation of Silicon Solar Cells Using Amorphous Silicon Carbid Layers. Photovoltaic Energy Conversion, Conference Record of the 2006 *IEEE 4th World Conference*, **2006**, 1016–1019.
9. Pandraud, G.; French, P. J.; Sarro, P. M. PECVD silicon carbide waveguides for multichannel sensors. *Sensors 2007, IEEE* **2007**, 395–398.
10. Zhang H.; Guo H.; Wang Y.; Zhang G.; Li Z. Study on PECVD SiC coated Pressure Sensor. *J. Micromechanics Microengi.* **2007**, *17*, 426–431.
11. Hui, G.; Yu, W.; Sheng, C.; et al. PECVD SiC as a Chemical Resistant Material in MEMS. NEMS '06, 1st *IEEE International Conference*, **2006**, 805–808.
12. Kakiuchi, H.; Ohmi, H.; Aketa, M.; Yasutake, K.; Yoshii, K.; Mori, Y. Effect of hydrogen on the structure of high-rate deposited SiC on Si by atmospheric pressure plasma chemical vapor deposition using high-power-density condition. *Thin Solid Films* **2006**, *496*, 259–265.
13. Losurdo, M.; Giangregorio, M.; et al. Structural and optical investigation of plasma deposited silicon carbon alloys: Insights on Si-C bond configuration using spectroscopic ellipsometry. *J. Appl. Phys.* **2005**, *97*, 103504.
14. Tauc, R. G.; Vancu, A. Optical properties and electronic structure of amorphous germanium. *Phys. Status Solidi.* **1966** *15*, 627–637.
15. Taraschewski, M.; Cammenga, H. K.; Tuckermann, R.; Bauerecker, S. FTIR study of CO_2 and H_2O/CO_2 nanoparticles and their temporal evolution at 80 K. *J. Phys. Chem.* **2005**, *109*, 3337–3343.
16. Tokmoldin, S. Zh.; Mukashev, B. N. Defects agglomeration in the vicinity of hydrogen-related vacancy-type complexes in proton-implanted silicon. *Mukashev, Physi. B: Condensed Matter* **2001**, *308*, 167–170.
17. Garcia, B.; Estrada, M. Influence of deposition conditions of a-Si1-xCx on film composition before and after excimer laser anneal. 6th International Caribbean Conference on Devices, Circuits and Systems, *IEEE*, **2006**, 157–160.
18. Goldie, D. M.; Persheyev, S. K. Quantitative hydrogen measurement in PECVD and HWCVD a-Si:H using FTIR spectroscopy. *J. materi. sci.* **2006**, *41*, 5287–5291.
19. Fujii, T.; Yoshimoto, M.; et al. Bonding structures in highly photoconductive a-SiC:H films deposited by hybrid-plasma chemical vapor deposition. *J. Non-Crystalline Solids* **1996**, *198–200*, 577–581.
20. Wang, L.; Huang, X.; Ma, Z.; Li, Z.; et al. Thermal anneal of a-Si:H/a-SiN_x:H multilayers. *Appl. Physi. A* **2002**, *74*, 783–786.
21. Li, Y.-M.; Anna Selvan, J. A.; et al. A study of single chamber RF-PECVD /spl mu/c-Si solar cells. 3rd World Conference on Photovoltaic Energy Conversion, *IEEE*, **2003**, 1788–1791.
22. Burton, J. C.; Sun, L.; Pophristic, M.; et al. Spatial characterization of doped SiC wafers by Raman spectroscopy. *J. Appl. Phys.* **1988**, *84*, 6268–6273.
23. Baba, K.; Hatada, R. Preparation of diamond-like carbon films by plasma source ion implantation with superposed pulse. Ion Implantation Technology Conference, *IEEE*, **2000**, 512–514.
24. Moulder, J. F.; Stickle, W. F.; Sobol, P. E.; Bomber, K. D. Handbook of X-ray Photoelectron Spectroscopy, Eden Prairie, Perkin-Elmer Corp., **1992**.
25. Wijesundara, M. B. J.; Valente, G.; Ashurst, W. R.; et al. Single-source chemical vapor deposition of 3C-SiC films in a LPCVD reactor I. Growth, structure, and chemical characterization. *J. Electrochemical Soc.* **2004**, *151*, C210–C214.
26. Kawabe, T.; Tabata, K.; Suzuki, E.; et al. Photoemission study of the subsequential oxidation of dissociatively adsorbed methane on an SnO_2 thin film. *Surf. Interface Anal.* **2000**, *29*, 791–797.
27. Le Normand, F.; Hommet, J.; Szörényi, T.; Fuchs, C.; Fogarassy, E. XPS study of pulsed laser deposited CN*x* films. *Physi. Review B* **2001**, *64*, 235416 [15 pages].